ARTICLE IN PRESS

ELSEVIER

Cardiovascular Research 1 (2002) 000–000

Cardiovascular Research

www.elsevier.com/locate/cardiores

Endocardial versus epicardial differences in L-type calcium current in canine ventricular myocytes studied by action potential voltage clamp

Tamás Bányász[a], László Fülöp[a], János Magyar[a], Norbert Szentandrássy[a], András Varró[b], Péter P. Nánási[a,*]

[a]Department of Physiology, University Medical School of Debrecen, P.O. Box 22, H-4012 Debrecen, Hungary
[b]Department of Pharmacology and Pharmacotherapy, University of Szeged, P.O. Box 427, H-6701 Szeged, Hungary

Received 24 May 2002; accepted 10 December 2002

Abstract

Objectives: The aim of the present study was to assess and compare the dynamics of L-type Ca^{2+} current ($I_{Ca,L}$) during physiologic action potential (AP) in canine ventricular cardiomyocytes of epicardial (EPI) and endocardial (ENDO) origin. **Methods:** $I_{Ca,L}$ was recorded on cells derived from the two regions of the heart using both AP voltage clamp and conventional whole cell voltage clamp techniques. **Results:** AP voltage clamp experiments revealed that the decay of $I_{Ca,L}$ is monotonic during endocardial AP, whereas the current is double-peaked (displaying a second rise) during epicardial AP. The amplitude of the first peak was significantly greater in ENDO (-4.6 ± 0.8 pA/pF) than in EPI cells (-2.8 ± 0.3 pA/pF). Application of epicardial APs as command pulses to endocardial cells yielded double-peaked $I_{Ca,L}$ profiles, and increased the net charge entry carried by $I_{Ca,L}$ during the AP from 0.187 ± 0.059 to 0.262 ± 0.056 pC/pF ($n=5$, $P<0.05$). No differences were observed in current densities and inactivation kinetics of $I_{Ca,L}$ between EPI and ENDO cells when studied under conventional voltage clamp conditions. Nisoldipine shortened action potentials and eliminated the dome of the epicardial AP. **Conclusion:** $I_{Ca,L}$ was shown to partially inactivate before and deactivate during phase-1 repolarization and reopening of these channels is responsible for the formation of the dome in canine EPI cells. The transmural differences in the profile of $I_{Ca,L}$ could be well explained with differences in AP configuration.

Keywords: Ca-channel; Ion channels; Membrane currents; Membrane potential; Myocytes

1. Introduction

There are well-known differences in the configuration of the AP of cardiomyocytes originating from various layers of the ventricular wall in mammalian myocardium [1,2]. These differences are generally attributed to asymmetrical distribution of various potassium currents, like I_{to}, I_{Kr}, I_{Ks} and I_{K1} [3–7]. The transmural heterogeneity in AP configuration is probably most prominent in canine ventricular myocytes, where endocardial (ENDO) APs exhibit a prominent plateau, while a spike-and-dome appearance is characteristic to APs recorded from the epicardial (EPI) cells [1,3,8,9]. It is now well established that the greater density of I_{to} measured in canine EPI cells is responsible for the prominent spike-and-dome configuration of the AP, whereas I_{to} was found to be less accentuated in ENDO myocytes in accordance with the monotonic phase-2 repolarization, absence of the incisura, and longer AP duration in ENDO cells [1,3]. While previous studies focused on the transmural heterogeneity of repolarizing currents, no relevant study on $I_{Ca,L}$ was performed. This prompted us to investigate the transmural heterogeneity of the kinetic properties of $I_{Ca,L}$ in EPI and ENDO canine ventricular myocytes.

We have several reasons to anticipate EPI–ENDO differences in the performance of $I_{Ca,L}$. Differences in AP configuration may influence $I_{Ca,L}$ through its voltage-dependency. The transmural gradient for both systolic and diastolic $[Ca^{2+}]_i$ may also modify inactivation kinetics of

*Corresponding author. Tel.: +36-52-416-634; fax: +36-52-432-289.
E-mail address: nanasi@phys.dote.hu (P.P. Nánási).

Time for primary review 26 days.

0008-6363/02/$ – see front matter
doi:10.1016/S0008-6363(02)00853-2

the current [10]. Furthermore, mathematical simulation of $I_{Ca,L}$ predicted rapid activation and subsequent partial inactivation of the current during an AP including the possibility of reopening of the channels [11]. To test these predictions we applied the combination of the conventional whole-cell voltage clamp and AP voltage clamp techniques. This latter method offers a valuable approach to study the dynamics of a specific ion current as it is actually displayed during the cardiac AP [12–14]. The aim of the present study was: (1) to assess the profile of $I_{Ca,L}$ during physiologic AP in canine cardiomyocytes, (2) to compare the dynamics of $I_{Ca,L}$ in ENDO and EPI myocytes, and (3) to decide whether the observed differences are attributable to differences in AP configuration in the two regions.

2. Methods

2.1. Isolation of single canine ventricular myocytes

Adult mongrel dogs of either sex were anesthetized with intravenous injections of 10 mg/kg ketamine hydrochloride (Calypsolvet, SelBruHa Kft., Hungary)+1 mg/kg xylazine hydrochloride (Rometar, Alfasan, The Netherlands). The hearts were quickly removed in deep anesthesia and placed in Tyrode solution. The entire investigation conformed to the *Guide for the Care and Use of Laboratory Animals* published by the US National Institutes of Health, as well as the principles outlined in the Declaration of Helsinki. Single myocytes were obtained by enzymatic dispersion using the segment perfusion technique [15,16]. Briefly, a wedge-shaped section of the ventricular wall supplied by the left anterior descending coronary artery was dissected, cannulated and perfused with oxygenated Tyrode solution containing: NaCl 144, KCl 5.6, $CaCl_2$ 2.5, $MgCl_2$ 1.2, HEPES 5, and dextrose 11 mM at pH 7.4. Perfusion was maintained until the removal of blood from the coronary system and then switched to a nominally Ca^{2+}-free Joklik solution (Minimum Essential Medium Eagle, Joklik Modification, Sigma) for 5 min. This was followed by 30-min perfusion with re-circulated Joklik solution supplemented with 1 mg/ml collagenase (Type II, Worthington Chemical) and 0.2% bovine serum albumin (Fraction V, Sigma) containing 50 μM Ca^{2+}. Portions of the left ventricular wall having EPI or ENDO origin were cut into small pieces and the cell suspension obtained at the end of the procedure was washed with Joklik solution and the Ca^{2+} concentration was gradually increased to 2.5 mM. The cells were stored in Minimum Essential Medium Eagle supplemented with taurine (20 mM), pyruvic acid (2 mM), ribose (5 mM), allopurinol (0.1 mM), $NaHCO_3$ (26 mM) and NaH_2PO_4 (1.5 mM) at 14 °C until use.

2.2. Electrophysiology

The whole-cell configuration of the ruptured patch clamp technique [17] was used for all recordings. Myocardial cells were transferred to a thermoregulated chamber (0.5 ml volume) mounted on the stage of an inverted microscope and superfused with Tyrode solution. All experiments were performed at 37 °C. The flow rate was 10 ml/min. Electrodes were prepared from borosilicate glass, having a tip resistance of 1.5–2.5 MΩ when filled with pipette solution (containing: K-aspartate 100, KCl 45, $MgCl_2$ 1, EGTA 10, K-ATP 3, and HEPES 5 mM, for AP voltage clamp, or KCl 110, KOH 40, TEACl 20, HEPES 10, K-ATP 3, EGTA 10, and GTP 0.25 mM for conventional voltage clamp experiments, at pH 7.4). Careful suction was applied to help gigaseal formation and the subsequent disruption of the membrane patch. Axoclamp 2B amplifier (Axon Instruments) was used in current clamp or continuous single electrode voltage clamp mode. The output filter was set to 10 kHz. Digidata 1200 A/D–D/A converter operated under pClamp 6.0 software (Axon Instruments) was used to collect data and to deliver voltage clamp protocols. Ionic currents were normalized to cell capacitance, determined in each cell using hyperpolarizing pulses from −10 to −20 mV for 40 ms. The mean value for cell capacitance was 142±5.4 pF. The series resistance was typically 4–8 MΩ before compensation (usually 50–80%). In conventional voltage clamp experiments $I_{Ca,L}$ was measured during 200-ms-long depolarizations to +10 mV arising from the holding potential of −40 mV. Peak current density was defined as a difference between the peak value of $I_{Ca,L}$ and its pedestal measured at the end of the pulse. The time constant of current decay (inactivation) was fitted as a sum of two exponential components. The voltage-dependence of steady-state inactivation was determined using test depolarizations to +10 mV preceded by a set of prepulses clamped to various voltages between −55 and +20 mV for 500 ms. Peak currents measured after these prepulses were normalized to the peak current measured after the −55 mV prepulse and plotted against the respective prepulse potential. Data were fitted to the two-state Boltzmann function.

In AP voltage clamp studies, the AP waveform was first recorded from the cell in current clamp mode applying steady-state stimulation at a cycle length of 1 s and stored on the hard disk. This record was transformed to command file using laboratory-made software, then delivered as the command voltage in voltage clamp mode. In this case the current trace was a horizontal line at the zero level. Application of 1 μM nisoldipine (Bayer, Leverkusen, Germany) for 2 min dissected $I_{Ca,L}$ with an inverse polarity [18]. In our graphs this nisoldipine-sensitive current was displayed so as to appear as an inwardly directed current.

2.3. Statistics

Results are expressed as mean±S.E.M. values. The statistical significance of differences among groups was evaluated with one-way ANOVA followed by Bonferroni

test. Differences were considered significant when P was less than 0.05.

3. Results

3.1. Comparison of $I_{Ca,L}$ profile in ENDO and EPI canine myocytes using AP voltage clamp

The time course of $I_{Ca,L}$ during the AP was determined as nisoldipine-sensitive current using the AP voltage clamp method (Fig. 1). $I_{Ca,L}$ exhibited a sharp spike and rapid decay in both ENDO and EPI cells. Activation of $I_{Ca,L}$ was apparently faster when recorded under AP clamp conditions comparing to conventional voltage clamp measurements. This can be attributed to the rapid development of the early repolarization (phase 1) of the AP preventing full activation of $I_{Ca,L}$. Following the spike a hump was developed on the $I_{Ca,L}$ in EPI but not in ENDO cells. This hump, or second peak, arose following the deepest point of the incisura of the AP and reached its maximum before the top of the dome. The amplitude of the first peak was

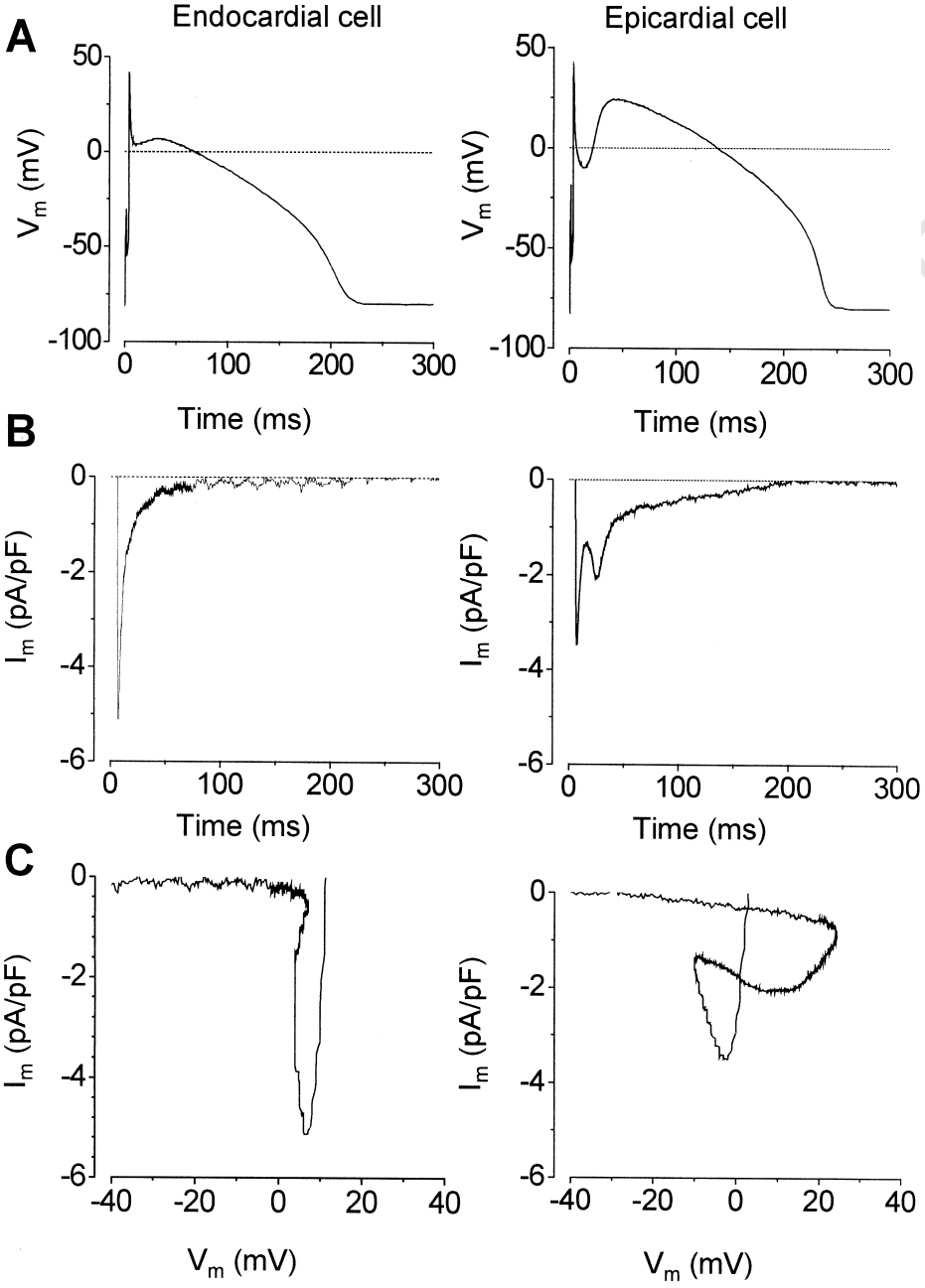

Fig. 1. Representative action potentials (A), $I_{Ca,L}$ profiles (B), and current–voltage relationships (C) recorded under AP voltage clamp conditions in ENDO (left panels) and EPI (right panels) cells of canine ventricular myocardium. $I_{Ca,L}$ was measured as nisoldipine-sensitive current, the initial 2–2.5 ms of the record was distorted by the poorly controlled I_{Na}, thus it was omitted from the graph. Current–voltage relationship for $I_{Ca,L}$ was obtained by plotting the nisoldipine-sensitive current against isochronal membrane potential values derived from the AP.

significantly greater in ENDO than in EPI cells (-4.6 ± 0.8 vs. 2.8 ± 0.3 pA/pF, respectively, $P<0.05$). The amplitude of this second peak (observed exclusively in EPI cells) was smaller than the first one in each cell examined. The current–voltage relationship of $I_{Ca,L}$ (displayed as phase-plane trajectories in Fig. 1C) indicates that the current built up within a narrow range of membrane potential, then the current began to fall in both types of cells. This decline was monotonic and complete in ENDO cells, whereas the second rise of $I_{Ca,L}$ formed a second loop on the I–V relationship around $+10$ mV in EPI myocytes. After this there was a continuous decrease in $I_{Ca,L}$ during the plateau of the AP, and the nisoldipine-sensitive current was less than 50 pA at potentials negative to 0 mV. It must be noted, however, that no sustained current was recorded during the plateau in ENDO cells, in contrast to the slowly declining but non-zero current flowing during the dome of EPI myocytes. Similar results were obtained in the 14 EPI and 10 ENDO cells studied.

The question arises whether the kinetic properties of L-type Ca^{2+} channels located in the membrane of EPI and ENDO myocytes may be different, or alternatively, the differences observed in the $I_{Ca,L}$ profiles are due to differences in the AP configuration. To answer this question the following experiment was performed. Using the own AP of an ENDO cell as a voltage command, the $I_{Ca,L}$ profile recorded during AP voltage clamp was characteristic naturally to that of ENDO cells (Fig. 2A). When an AP having identical duration, but recorded in a previous experiment from an EPI cell, was applied as voltage command to the ENDO cell, the $I_{Ca,L}$ profile became similar to that recorded from the EPI cell, i.e. the second hump on the falling limb of $I_{Ca,L}$ appeared (Fig. 2B), and the current–voltage relationship displayed the two loops configuration (not shown). Similar results were observed in all the five ENDO cells, each exposed to its own and a matching EPI AP as voltage command. The area under $I_{Ca,L}$ was calculated in order to assess the net charge influx through the L-type channels under these experimental conditions (Fig. 2C). The net charge entry, carried by $I_{Ca,L}$ during the AP, was significantly greater when applying EPI APs instead of the own ENDO APs of the cells (0.262 ± 0.056 vs. 0.187 ± 0.059 pC/pF, $n=5$, $P<0.05$). These results suggest that the characteristic ENDO- or EPI-like $I_{Ca,L}$ profile is not determined by the actual origin of the cell but is a strict consequence of the configuration of the AP experienced. The calculations also indicate that Ca^{2+} influx may be higher in EPI than ENDO cells, again due to differences in AP configuration, and may probably—at least in part—account for the higher systolic and diastolic intracellular Ca^{2+} concentrations found in EPI versus ENDO myocytes [10].

3.2. Kinetic properties of $I_{Ca,L}$ under conventional voltage clamp

The results shown in Fig. 2 suggest that the EPI-ENDO differences observed in AP voltage clamp experiments are likely consequences of differences in AP configuration. This conclusion can be drawn only after direct comparison of the properties of $I_{Ca,L}$ in EPI and ENDO canine myocytes under conventional voltage clamp conditions. In these experiments I_{to} was blocked by 3 mM 4-aminopyridine added to the bathing solution, and $I_{Ca,L}$ was activated by a series of 200-ms-long depolarizations to test potentials increasing in 5 mV steps from -35 to $+60$ mV. The current–voltage relationships constructed from these data (not shown) were fully identical in case of EPI and ENDO cells: the current first appeared at -20 mV, its peak value was reached at $+10$ mV, and the reversal potential was obtained at $+50$ mV. Similarly, no significant differences were observed between the EPI ($n=5$) and ENDO ($n=6$) myocytes when comparing peak density of $I_{Ca,L}$ (-4.93 ± 1.15 vs. -4.63 ± 0.75 pA/pF, $P=0.42$), the midpoint potential of steady-state inactivation (-15.9 ± 0.34 vs. -15.1 ± 0.57 mV, $P=0.21$), or its slope factor (3.45 ± 0.3 vs. 3.39 ± 0.24 mV, $P=0.47$).

To explain the mechanism of the second activation of $I_{Ca,L}$, observed in canine EPI cells under AP voltage clamp, we assumed that part of $I_{Ca,L}$ deactivates during the early repolarization (phase-1) of the AP and this population of deactivated channels may reopen during the crest of the dome in EPI cells. Also, another fraction of $I_{Ca,L}$ which has already been inactivated before the early repolarization may recover from inactivation during the incisura. To test this hypothesis the voltage-dependence of deactivation and recovery from inactivation of $I_{Ca,L}$ was studied using paired pulse protocols.

In the first series of these experiments (Fig. 3A–C) two depolarizing pulses (P_1 and P_2, having durations of 25 and 100 ms, respectively) were delivered from -40 to $+10$ mV at a cycle length of 5 s, with varying the interpulse potential. The underlying current records show the $I_{Ca,L}$ elicited by the first pulse then interrupted by repolarizing steps (Fig. 3A). Note that, in spite of the increased driving force for $I_{Ca,L}$, the current failed to increase during the repolarizing pulses, in contrast, the current fell to values close to zero rapidly after decaying of the capacitive transient, presumably due to voltage-dependent deactivation. The voltage-dependence of this deactivation is shown in Fig. 3B, obtained by plotting the current measured at the end of the interpulse interval (I_r) and normalized to the peak current during the first pulse (I_{P1}) against the respective interpulse potential. Results were fit to a two-state Boltzmann function yielding a midpoint potential of -12.7 ± 1 mV and a slope factor of 6.5 ± 1 mV in six experiments. These results indicate that substantial amount of deactivation of $I_{Ca,L}$ can be anticipated at the membrane potential range covered by the incisura.

According to our assumption the pool of calcium channels that may reopen during the second depolarization is composed of channels which closed via deactivation during the interpulse interval plus those closed via inactivation during the first pulse. Fig. 3C illustrates the

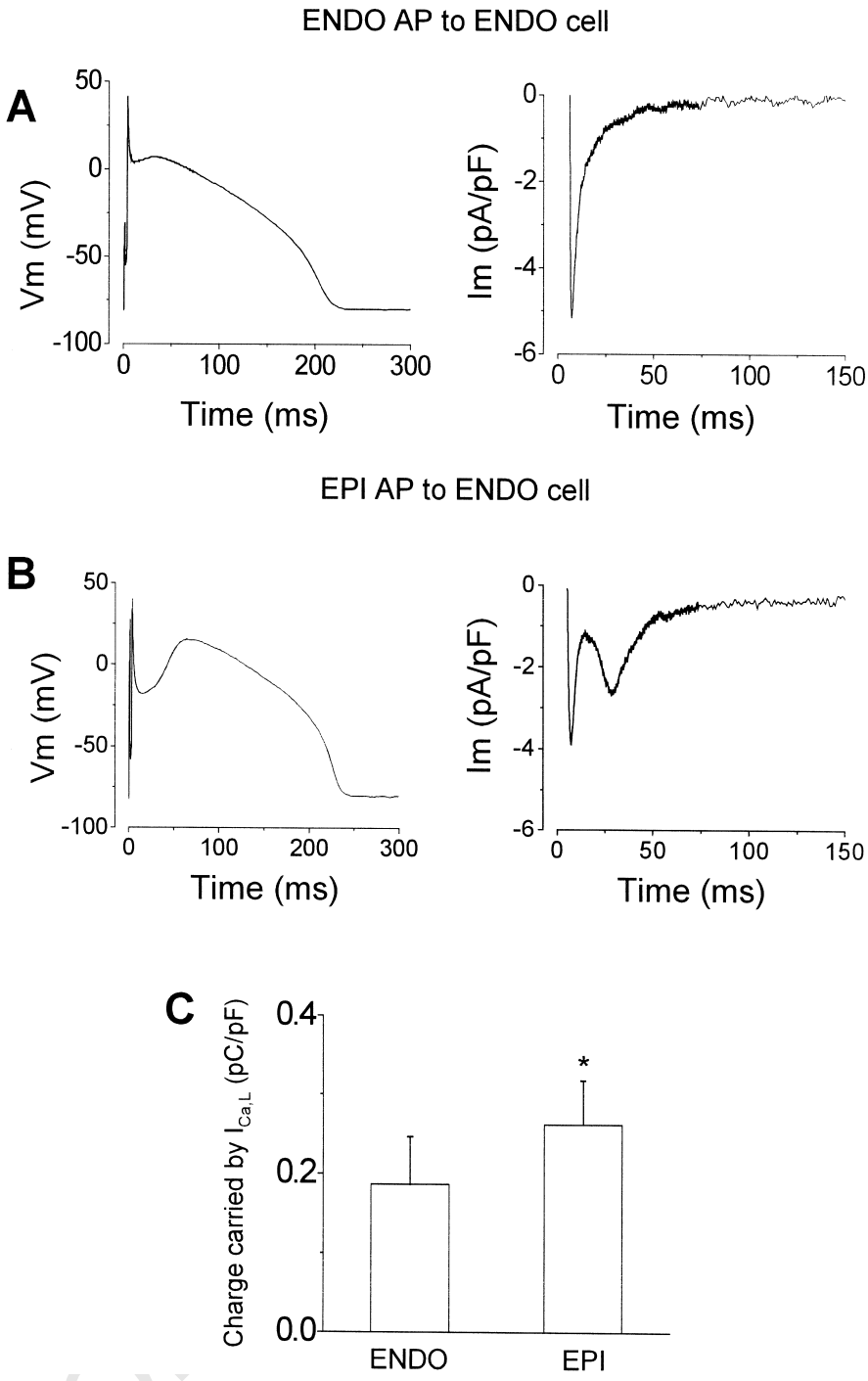

Fig. 2. Influence of AP configuration (left) on the $I_{Ca,L}$ profile (right) recorded from a canine ENDO cell under AP voltage clamp conditions. In panel A the own AP of the cell was applied as voltage command, while in panel B an AP having identical duration, but recorded in a previous experiment from an EPI cell, was delivered as command signal to the ENDO cell. Panel C displays the net charge entry, calculated by integration of the $I_{Ca,L}$ profile during the AP in five ENDO cells using both ENDO and EPI APs as voltage commands. Columns and bars represent mean±S.E.M. values, asterisk denotes the level of significance ($P<0.05$).

relation between the interpulse potential and the peak amplitude of $I_{Ca,L}$ measured during the second pulse (I_{P2}) normalized to I_{P1}. With increasing the hyperpolarizing voltage prior to the second depolarization, the peak amplitude of $I_{Ca,L}$ increased in a voltage-dependent manner. Lengthening the interpulse interval from 25 to 100 ms also increased the amplitude of the second peak of $I_{Ca,L}$ indicating an increasing contribution of previously inactivated and reopening Ca^{2+} channels to the second current peak. The availability of $I_{Ca,L}$ reached 89.6±2% of I_{P1} when applying interpulse duration of 100 ms and an interpulse potential of −40 mV. The voltage-dependence of recovery from inactivation can be best assessed by plotting the I_{P2}/I_{P1} ratios as a function of the interpulse

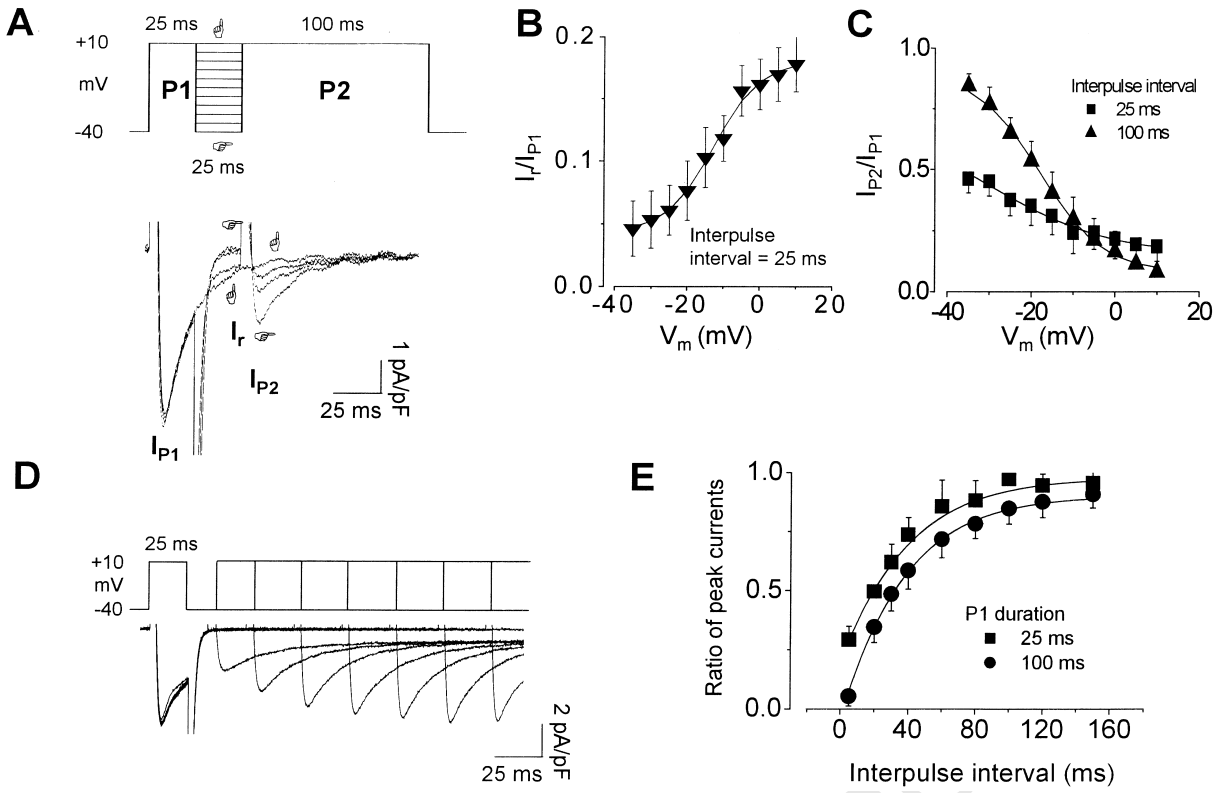

Fig. 3. (A–C) Evidence for voltage-dependent deactivation and voltage-dependent reopening of the deactivated and inactivated L-type Ca^{2+} channels in canine ventricular myocytes. Two rectangular depolarizing voltage pulses (P_1 and P_2, having durations of 25 and 100 ms, respectively) were delivered to +10 mV from the holding potential of −40 mV (A). These pulses were separated by either a 25 or 100 ms long interpulse interval, clamped to potentials ranging between −40 and +10 mV. The current peaks measured during P_1 and P_2 are I_{P1} and I_{P2}, respectively, and the current measured at the end of the interpulse interval was termed as I_r. Ratios of I_r/I_{P1} (B) and I_{P2}/I_{P1} (C) were plotted as a function of the interpulse potential to describe the voltage-dependence of deactivation and recovery from inactivation, respectively. Solid lines were obtained by fitting data to a two-state Boltzmann function. Panel E shows the time course for recovery from inactivation of $I_{Ca,L}$, measured using a twin-pulse protocol (D), where the duration of the first pulse was either 25 or 100 ms. The interpulse interval was gradually increased up to 150 ms. The peak current measured during the second pulse was normalized to that measured during the first one and these current ratios were plotted in the ordinate as a function of the interpulse interval. Solid lines represent fits to single exponentials. Symbols and bars are mean±S.E.M. values obtained in six cells.

potential using the longer (100 ms) interpulse interval. Fitting the results to the two-state Boltzmann function yielded a midpoint potential of −18.0±0.8 mV and a slope factor of 7.5±0.8 mV in six experiments. Measurements using the shorter (25 ms) interpulse interval were performed simply to demonstrate that the availability of $I_{Ca,L}$ will increase with the degree of repolarization during the incisura of the AP (i.e. under conditions simulating the spike-and-dome configuration of the EPI AP).

The time course of recovery from inactivation of $I_{Ca,L}$ was determined using the twin-pulse protocol shown in Fig. 3D. The interpulse interval, following the first depolarization having either 25 or 100 ms in duration, was continuously varied from 5 to 150 ms. The shorter (25 ms) prepulse was applied to approximate conditions occurring during an AP, while the longer (100 ms) prepulse was used to fully inactivate the current allowing the determination of its recovery time constant. The ratio of peak currents (I_{P2}/I_{P1}) was plotted against the interpulse interval and the time constant for recovery was estimated by fitting data with a single exponential (Fig. 3E). The time constant for recovery of $I_{Ca,L}$, estimated after 100 ms prepulses, was 37.2±1.2 ms and the maximum ratio of I_{P2}/I_{P1} was 0.92±0.01 in the six myocytes studied. Again, it is important to note that the recovery curve obtained using 25 ms prepulse duration started from a non-zero value indicating that a fraction of channels (which failed to inactivate within the 25 ms duration of the prepulse, consequently, closed via deactivation after the prepulse) was available for activation immediately after the prepulse. Fig. 3E also suggests that the fraction of $I_{Ca,L}$ available for activation during the crest of the dome of the AP will increase with increasing the duration of the incisura.

3.3. Relationship between $I_{Ca,L}$ profile and AP configuration

In the voltage clamp experiments above, rectangular voltage protocols were applied to mimic the membrane potential changes during the AP and study the voltage- and

time-dependent behavior of $I_{Ca,L}$. The results predict that a longer and deeper incisura increases the probability of later reopenings of Ca^{2+} channels, implicating that timing of the AP and the profile of $I_{Ca,L}$ may be coupled. To show the temporal relationship between the AP and $I_{Ca,L}$, the time to the maximum rate of depolarization during the dome of AP ($t_{V_{max}}$ dome) was plotted as function of the time to the maximum value of the second calcium peak ($t_{I_{Ca}}$ peak), both measured from the upstroke of the AP in EPI cells. The correlation between these parameters was highly linear in the nine myocytes examined (Fig. 4A). This observation indicates that the development of the dome of AP and the second peak of $I_{Ca,L}$ are linked tightly in EPI cells, raising the possibility that the second peak on $I_{Ca,L}$ may provide the depolarizing current responsible for the formation of the dome. To investigate this point further we compared the time course of the double-peaked $I_{Ca,L}$ with the net membrane current (I_{net}) calculated from the AP in EPI cells [19]. I_{net} was estimated as the product of the membrane capacitance and the first time-derivative of the AP ($I_{net} = -C_m \times dV/dt$). The result of a representative experiment is presented in Fig. 4B, where an excellent overlap is shown between I_{net} and the nisoldipine-sensitive current during the crest of the dome, however, the currents diverged during phase-2 and phase-3 repolarization. This overlap means that the net membrane current is dominated by $I_{Ca,L}$ at this period of the AP. Similar observations were obtained in five canine cells.

If the dome formation of the EPI AP is really coupled to a second activation of $I_{Ca,L}$, then suppression of this current must eliminate the dome. Fig. 4C displays the effect of nisoldipine (1 μM) on the morphology of an EPI AP. Superfusion of the cells with nisoldipine resulted immediately in depression of plateau, loss of the spike-and-dome configuration and significant shortening of AP (from 215±16 to 105±8 ms, $P<0.001$, $n=7$). These profound changes, limited to phase-2 and phase-3 of the AP, were strictly associated, i.e. we never found cells with depressed plateau without significant shortening of AP, or shortened AP with intact dome, thus loss of $I_{Ca,L}$ is presumably responsible for both elimination of the dome and the resultant shortening of AP. These results confirm our hypothesis that the dome of the EPI AP is indeed due to the rise of the second $I_{Ca,L}$ peak.

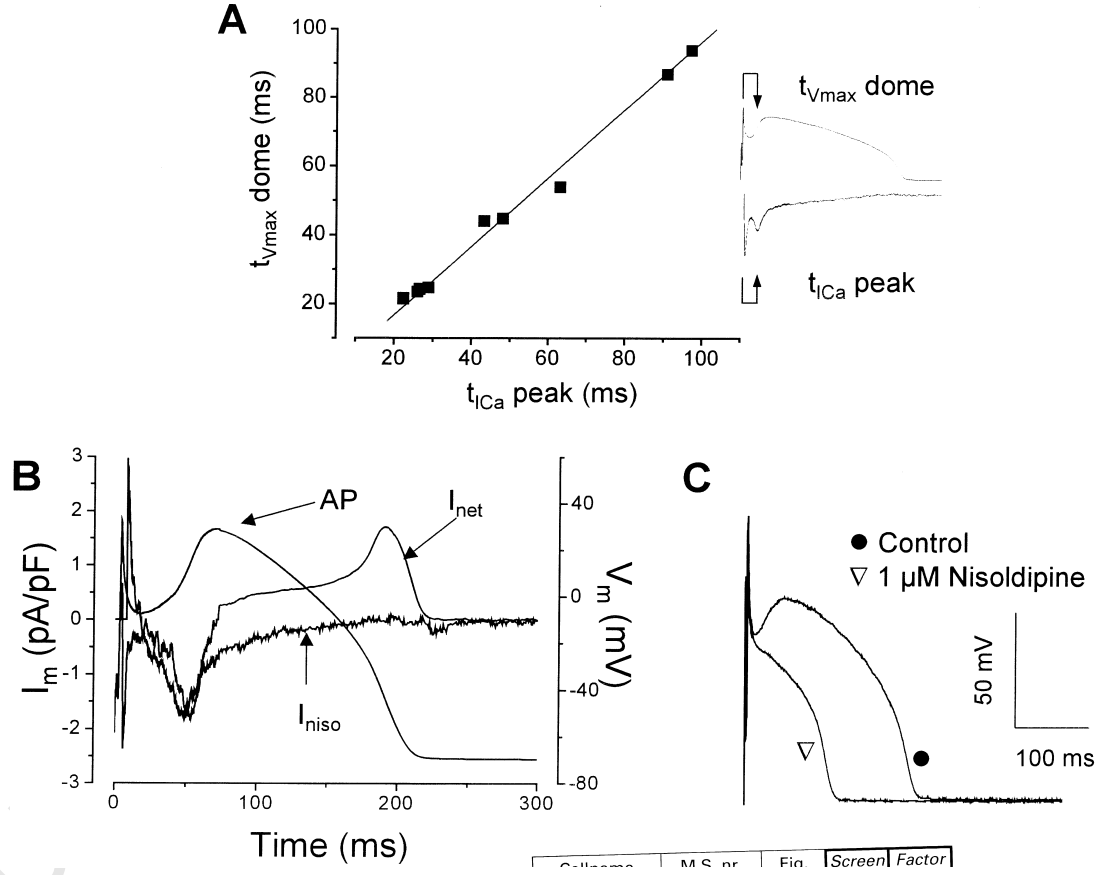

Fig. 4. (A) Correlation between the time to the second peak of the nisoldipine-sensitive current ($t_{I_{Ca}}$ peak) and time to maximum rate of depolarization of the dome ($t_{V_{max}}$ dome), both measured from the upstroke of the AP in nine canine EPI cells. Linear regression (solid line) yielded a value for $r^2>0.98$. (B) Comparison of the profile of the nisoldipine-sensitive current (I_{niso}) and the net membrane current (I_{net}) during the AP of an EPI cell. I_{net} was estimated as the product of the membrane capacitance and the first time-derivative of the AP ($I_{net} = -C_m \times dV/dt$). (C) Action potentials recorded before and 5 s after the superfusion of an EPI myocyte with 1 μM nisoldipine.

3.4. Computer simulations

Finally, we modeled the time course of $I_{Ca,L}$ during ENDO and EPI APs. For computation of the $I_{Ca,L}$ profile we used kinetic parameters published by Luo and Rudy [20] completed with the Kass–Sanguinetti inactivation kinetics [21]. Two canine APs, one of EPI and the other of ENDO origin, having equal durations at 90% repolarization, were selected from our records for modeling of $I_{Ca,L}$ and the phase-plane trajectories in the two cell types. Results are shown in Fig. 5. The Luo–Rudy model predicts the secondary hump on $I_{Ca,L}$ in EPI cells. The model also predicts that following the rapid activation of $I_{Ca,L}$ the current decays quickly with a very small sustained component during the plateau. This is consistent with our experimental observations regarding the time course of the nisoldipine-sensitive current during AP. The *I–V* relationship calculated from the model is highly consistent with the experimental results.

4. Discussion

Our study is first to demonstrate the marked differences existing in the $I_{Ca,L}$ profiles of ENDO and EPI canine ventricular myocytes using the AP clamp voltage technique. These differences cannot be accounted for by inherent properties of the Ca^{2+} channels in the two populations of cells because myocytes with ENDO origin displayed a double-peaked, EPI-like calcium current when EPI AP was applied as a command pulse under AP voltage clamp. Although the physiological role of AP configura-

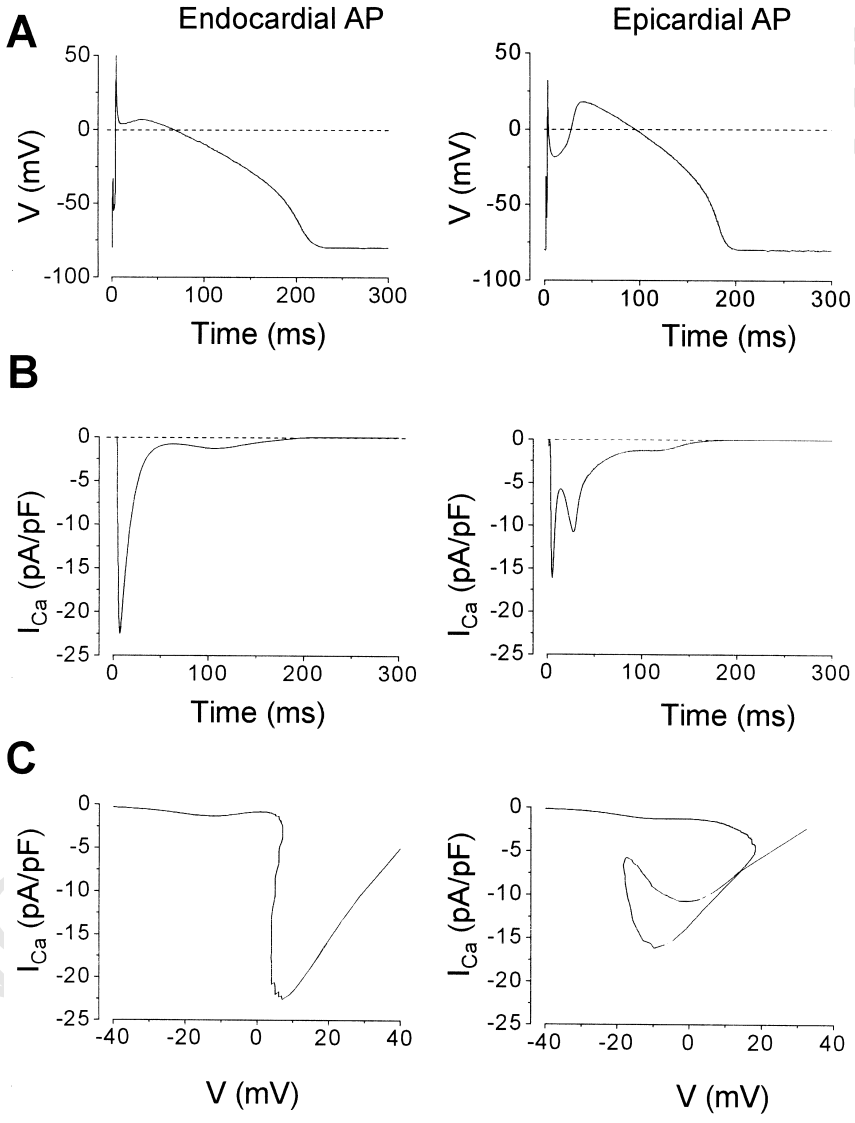

Fig. 5. $I_{Ca,L}$ profiles (B) and the corresponding current–voltage relations (C) computed for ENDO (left panels) and EPI (right panels) myocytes using the Luo–Rudy model, completed with Kass–Sanguinetti inactivation kinetics. Representative ENDO and EPI APs (A), having similar durations, were recorded previously from canine cells and inserted into the model.

tion in governing membrane currents is not fully understood, several reports were published on the impact of the AP configuration on $I_{Ca,L}$ profile. Early studies, based on traditional voltage clamp experiments using rectangular command pulses, concluded that an increased driving force due to early repolarization can maintain a sustained component of $I_{Ca,L}$ during the plateau. This prediction was justified experimentally under AP voltage clamp conditions in guinea pig and rabbit, however, the results were contradictory in the rat [12,22–24]. Arreola et al. also reported a sustained component of $I_{Ca,L}$ during the plateau of the AP in guinea pig ventricular cells, but, in contrast to our results, reactivation of $I_{Ca,L}$ was not detected in that study [12]. They proposed that the increased driving force for Ca^{2+}, resulting from partial repolarization during phase-1, as well as a partial inactivation and the subsequent voltage-dependent recovery from inactivation of $I_{Ca,L}$ at plateau potentials is responsible for the sustained $I_{Ca,L}$. Similar results and conclusions were drawn by Yuan et al. in rabbit [22], and by Linz and Meyer in guinea pig, rat and rabbit myocytes [23,24]. In contrast to these reports, the Luo–Rudy model predicts only a minor sustained component during canine ventricular AP [20]. Indeed, in our experiments performed in canine cardiomyocytes, no sustained component was observed in ENDO cells, and only a small sustained $I_{Ca,L}$ was found in EPI cells during the plateau. From this point of view our results are in accordance with those of Zygmunt et al. [25], and Volk et al. [26] who found no sustained component of $I_{Ca,L}$ in canine and rat myocardium. These results suggest that the configuration of AP controls the $I_{Ca,L}$ profile during the AP, and due to the well-known interspecies heterogeneity in AP configuration, serious interspecies differences in the $I_{Ca,L}$ profile can be anticipated.

If—as our data demonstrate—shifting the membrane potential toward more negative values does not increase $I_{Ca,L}$ during canine AP, what is the consequence of the early repolarization regarding $I_{Ca,L}$? Present results might provide some insight into the behaviour of canine cardiac L-type Ca^{2+} channels during the AP. The results indicate that the primary consequence of early repolarization is voltage-dependent deactivation of L-type Ca^{2+} channels (i.e. closure of the channel due to closure of the activation gate). The fraction of channels driven into the deactivated state is primarily determined by the depth of the incisura as well as the time elapsed before the deepest point of the incisura. Another population of Ca^{2+} channels, that may contribute to the development of the dome, when reopening, represent those channels which had already been inactivated (i.e. became closed via closure of the inactivation gate) before the early repolarization and thus may recover from inactivation during the incisura. The number of these channels depends on the depth and duration of the incisura. Our experiments, using rectangular voltage pulses to simulate this constellation, suggest that a deeper and longer incisura may yield a larger population of Ca^{2+} channels ready to reopen during the dome. The large incisura (followed by the dome) in canine EPI myocytes fulfils the requirements above due to the large density of I_{to} in these cells [1,3,8,9].

According to our results the second peak of $I_{Ca,L}$ strictly coincided with the crest of the dome in canine EPI myocytes suggesting a casual relationship between the rise of this second current peak and development of the dome. The timing of the early plateau is known to be determined by a fine balance of I_{to} and $I_{Ca,L}$. When $I_{Ca,L}$, due to its slower inactivation, overwhelms I_{to}, the membrane potential reaches its inflection point and phase-1 repolarization is followed by a second depolarization. Acceleration of this second depolarization is due to reopening of Ca^{2+} channels as a consequence of their positive feedback control (in a manner similar to the Hodgkin cycle in the case of fast I_{Na}). Finally, inactivation of $I_{Ca,L}$ and activation of delayed potassium currents together with other currents activated during the plateau will determine the height and duration of the dome. The incisura is practically absent in ENDO cells, therefore, $I_{Ca,L}$ will monotonously inactivate throughout the plateau excluding the possibility of reopening. Thus, the major difference between the EPI and ENDO cells is that EPI cells do have a remarkable pool of Ca^{2+} channels available for a second activation, while ENDO cells do not. However, this difference is functional, and can be exclusively ascribed to the higher density of I_{to} in EPI cells, since no differences were observed between epicardial and endocardial $I_{Ca,L}$ under conventional voltage clamp conditions. Based on the experimental data we can propose a new model for generation of the early part of the cardiac AP. In this model the timing of $I_{Ca,L}$ is determined by the density of I_{to}. Such a relationship has already been proposed for I_{to} and I_{Cl} by Zygmunt et al. [25] in canine ventricular myocardium. Our results, together with Zygmunt's observations, clearly indicate that the physiological role of a membrane current can be evaluated only in context with the time course of the AP.

In this study we have shown that L-type Ca^{2+} channels can, in fact, reopen during a normal cardiac action potential. Such a mechanism has been proposed to be involved in generation of early afterdepolarizations [27–29]. Although we did not analyse EADs under AP clamp conditions, our results strongly support this hypothesis since EADs arise from membrane potentials more negative than the deepest point of the incisura seen in our EPI APs.

Acknowledgements

Financial support for the studies was obtained from grants to PPN and TB from the Hungarian Research Foundation (OTKA-T037332, OTKA-T037334), Hungarian Ministry of Health (ETT-244/2000), and Hungarian Ministry of Education (FKFP-0243/2000). Further support

was obtained from the National Research and Development Programs (NKFP-1A/0011/2002).

References

[1] Litovsky SH, Antzelevitch C. Transient outward current prominent in canine ventricular epicardium but not endocardium. Circ Res 1988;62:116–126.

[2] Stankovicova T, Szilard M, Scheerder ID, Sipido KR. M cells and transmural heterogeneity of action potential configuration in myocytes from the left ventricular wall of the pig heart. Cardiovasc Res 2000;45:952–960.

[3] Liu DW, Gintant GA, Antzelevitch C. Ionic bases for electrophysiological distinctions among epicardial, midmyocardial, and endocardial myocytes from the free wall of the canine left ventricle. Circ Res 1993;72:671–687.

[4] Liu DW, Antzelevitch C. Characteristics of the delayed rectifier current (I_{Kr} and I_{Ks}) in canine ventricular epicardial, midmyocardial and endocardial myocytes. A weaker I_{Ks} contributes to the longer action potential of the M cell. Circ Res 1995;76:351–365.

[5] Furukawa T, Kimura S, Furukawa N, Bassett AL, Myerburg RJ. Potassium rectifier currents differ in myocytes of endocardial and epicardial origin. Circ Res 1992;70:91–103.

[6] Brahmajothi MV, Campbell DL, Rasmusson RL et al. Distinct transient outward current (I_{to}) phenotypes and distribution of fast-inactivating potassium channel alpha subunit in ferret left ventricular myocytes. J Gen Physiol 1999;113:581–600.

[7] Wettwer E, Amos GJ, Posival H, Ravens U. Transient outward current in human ventricular myocytes of subepicardial and subendocardial origin. Circ Res 1994;75:473–482.

[8] Krishnan SC, Antzelevitch C. Sodium channel block produces opposite electrophysiological effects in canine ventricular epicardium and endocardium. Circ Res 1991;69:277–291.

[9] Litovsky SH, Antzelevitch C. Differences in the electrophysiological response of canine ventricular subendocardium and subepicardium to acetylcholine and isoproterenol. Circ Res 1990;67:615–627.

[10] McIntosh MA, Cobbe SM, Smith GL. Heterogeneous changes in action potential and intracellular Ca^{2+} in left ventricular myocyte sub-types from rabbits with heart failure. Cardiovasc Res 2000;45:397–409.

[11] DiFrancesco D, Noble D. A model of cardiac electrical activity incorporating ionic pumps and concentration changes. Phil Trans R Soc Lond B Biol Sci 1985;307:353–398.

[12] Arreola J, Dirksen RT, Shieh RC, Williford DJ, Sheu SS. Ca^{2+} current and Ca^{2+} transients under action potential clamp in guinea pig ventricular myocytes. Am J Physiol 1991;261:C393–C397.

[13] Doerr T, Denger R, Doerr A, Trautwein W. Ionic currents contributing to the action potential in single ventricular myocytes of the guinea pig studied with action potential clamp. Pflügers Arch 1990;416:230–237.

[14] Ibarra J, Morley GE, Delmar M. Dynamics of the inward rectifier K^+ current during the action potential of guinea pig ventricular myocytes. Biophys J 1991;60:1534–1539.

[15] Magyar J, Iost N, Körtvély Á et al. Effects of endothelin-1 on calcium and potassium currents in undiseased human ventricular myocytes. Pflügers Arch 2000;441:144–149.

[16] Bányász T, Magyar J, Körtvély Á et al. Different effects of endothelin-1 on calcium and potassium currents in canine ventricular cells. Naunyn Schmiedeberg's Arch Pharmacol 2001;363:383–390.

[17] Hamill OP, Marty A, Neher E, Sakmann B, Sigworth FJ. Improved patch-clamp techniques for high resolution current recording from cells and cell-free membrane patches. Pflügers Arch 1981;391:85–100.

[18] Zaza A, Rocchetti M, Brioschi A, Cantadori A, Ferroni A. Dynamic Ca^{2+}-induced inward rectification of K^+ current during the ventricular action potential. Circ Res 1998;82:947–956.

[19] Rocchetti M, Besana A, Gurrola GB, Possani LD, Zaza A. Rate dependency of delayed rectifier currents during the guinea-pig ventricular action potential. J Physiol 2001;534:721–732.

[20] Luo CH, Rudy L. A dynamic model of the cardiac ventricular action potential. Circ Res 1994;74:1071–1096.

[21] Kass RS, Sanguinetti MC. Inactivation of calcium channel current in the calf cardiac Purkinje fiber: evidence for voltage- and calcium-mediated mechanisms. J Gen Physiol 1984;84:705–726.

[22] Yuan W, Ginsburg KS, Bers DM. Comparison of sarcolemmal calcium channel current in rabbit and rat ventricular myocytes. J Physiol 1996;493:733–746.

[23] Linz KW, Meyer R. Control of L-type calcium current during the action potential of guinea-pig ventricular myocytes. J Physiol 1998;513:425–442.

[24] Linz KW, Meyer R. Profile and kinetics of the L-type calcium current during the cardiac ventricular action potential compared in guinea-pigs, rats and rabbits. Pflügers Arch 2000;439:588–599.

[25] Zygmunt AC, Robitelle DC, Eddlestone GT. I_{to1} dictates behavior of $I_{Cl(Ca)}$ during early repolarization of canine ventricle. Am J Physiol 1997;273:H1096–H1106.

[26] Volk T, Nguyen THD, Schultz JH, Ehmke H. Relationship between transient outward K^+ current and Ca^{2+} influx in rat cardiac myocytes of endo- and epicardial origin. J Physiol 1999;519:841–850.

[27] Wit AL, Rosen MR. Afterdepolarizations and triggered activity: distinction from automaticity as an arrhythmogen mechanism. In: Fozzard HA, Haber E, Jennings RB, Katz AM, Morgan HE, editors, The heart and cardiovascular system, New York: Raven Press, 1992, pp. 2148–2149.

[28] January CT, Riddle MJ, Salata JJ. A model for early afterdepolarizations: induction with the Ca^{2+}-channel agonist Bay K 8644. Circ Res 1988;62:563–571.

[29] January CT, Riddle MJ. Early afterdepolarizations: mechanism of induction and block; a role for L-type Ca^{2+} current. Circ Res 1990;64:977–990.